Chapter 2

Evolution of Meteoroids and the Formation of Meteoroid Streams

2.1 Introduction

The process of a meteoroid's release from a parent body and its subsequent evolution is a central component of this work. While we still simulate these general processes through numerical models and study in detail two specific meteoroid streams (the Perseids and Leonids), the general physical concepts involved deserve attention and review. In what follows we describe the basic evolution of a given meteoroid from its "birth" through to its existence as an independent solar system body. For specific examples we shall confine our attention to the Perseid and Leonid stream orbits, but emphasize that these are not representative of the numerous, low-inclination meteoroid streams which constitute the bulk mass of the meteoroid complex. More extensive reviews of the entire subject of meteoroid stream formation and evolution can be found elsewhere (cf. Williams, 1993; Ceplecha et al., 1998; Steel, 1994).

The basic processes involved are: (1) The cometary ejection of meteoroids; followed by (2) the change in the osculating orbit of the ejected meteoroid from the parent body; and (3) the meteoroid's evolution under the gravitational and radiation forces acting upon it after release.

2.2 Cometary Ejection of Meteoroids

The origin of meteoroids as solid bodies begins in the outer atmosphere of cooling giant stars (Red Giants) when silicate material condenses to form grains (Greenberg and Haige 1989). These grains form the seeds for interstellar dust particles, which populate the plane of our galaxy. Later, condensation of volatiles from gas in the interstellar medium on the silicate core produces small grains with an organic-refractory matrix as well as an icy outer layer. Due to gravitational instability in some portions of these dust "clouds", stars (and planets) may grow over time. Such star-forming regions are heavily populated with gas and dust from the earlier decay of other stars.

The formation of our solar system out of just such a cloud (the initial solar nebula) some 4.5 billion years ago consisted of a central condensation (the future sun) and a disk of solid material (from interstellar dust) of varying size interspersed with gas (cf. Weidenshilling, 1988 and references therein for a more detailed review). Out of this disk of planetesmals, the planets were formed as smaller material coagulated through the process of gravitational accretion and collisional sticking. However, not all of the planetesmals were utilized in the formation of the planets. A large number ($\sim 10^{15}$) of kilometre-sized (and larger) chunks of unprocessed material, essentially frozen interstellar gas and dust stuck together, remained as separate, independent bodies in the outer solar system.

These bodies were initially confined to the plane of the solar system (i.e. the ecliptic plane). Through subsequent interaction with the planets and stars passing by, some of these bodies were isotropically ejected from the interior (i.e. beyond the orbit of Saturn) parts of the solar system, while others beyond Neptune continued to orbit in the ecliptic plane in an extended disk out thousands of A.U. from the sun. Many were lost forever into interstellar space, but a large fraction of those which were scattered remained loosely bound to the solar system in a distant (<100 000 A.U.) spherical cloud.

Some of these icy bodies have remained bound to the Sun since its formation and are still present in the form of the Oort cloud (named after J. van Oort who first brought widespread attention to the probable existence of such a cloud). The icy bodies making up the Oort cloud are composed mainly of water ice (along with a small fraction of more

volatile ices, like CO and CH_4) and dust - the same interstellar dust which began the whole process. Never heated more than 100 K above absolute zero since their formation, these objects have been in “cold” storage for the last 4.5 billion years.

When perturbations from a passing star or galactic tides alter the large orbits of these icy bodies, some may be moved into smaller orbits, which bring them within the reach of planetary perturbations from the major planets, or into close contact with the terrestrial planets. Once this happens, many will be permanently ejected from the solar system but a fraction will also be more tightly captured and potentially driven closer to the sun through repeated, complex interactions with the planets.

Once these icy bodies get closer than ~3 A.U. to the sun, the radiation from the sun will sublimate water ice (and at a much further distance more volatile ices like CO). This process leads to the formation of an envelope of gas about the icy central body and expels, through gas drag, the interstitial dust grains near the nucleus. The smallest of these grains (~micron sized) are driven directly away from the sun by solar radiation pressure (see 2.3) to form a “tail”. As viewed from Earth at this point, the object looks like a fuzzy star with a tail which moves against the background stars - in literal translation “cometa” (Latin) meaning long-haired star - in its modern form, comet.

The majority of meteoroids are the products of cometary decay, both gradual and (occasionally) catastrophic. Whipple (1951) was the first to propose the modern model of a cometary nucleus - namely a homogenous collection of sand and ice - as a dirty snowball. Whipple also developed the equations dictating the velocity of ejection for a meteoroid of a given mass from a cometary nucleus. It is this initial ejection velocity which determines the starting orbit for the daughter meteoroids. While the details of meteoroid release from a cometary nucleus have been refined since Whipple’s time (cf. Finson and Probstein, 1968; Crifo and Rodinov, 1999), the basic physical picture remains intact.

As the nucleus approaches the Sun, the mass loss per unit time, Γ, is given by

$$\Gamma = \frac{\pi R_c^{\,2} S}{n r^2 H} \qquad (2.1)$$

where R_c is the radius of the comet, S the solar constant, r the heliocentric distance of the nucleus, H the mean heat of sublimation for the ice and $1/n$ is the fraction of incoming solar energy used for sublimation. At some distance l from the nucleus surface the pressure on a grain due to free molecular collisions is

$$P = \frac{\Gamma \bar{v}}{2\pi l^2} \tag{2.2}$$

where v is the mean molecule velocity and the sublimation is assumed to be confined to the sunward hemisphere and $l >> R_c$.

The outward drag force experienced by a meteoroid grain due to coma gas is given by

$$F_{drag} = \frac{C_d}{2} PA \tag{2.3}$$

where C_d is the drag coefficient (=26/9 for a sphere which re-emits impacting molecules with thermal speeds) and A is the cross-sectional area of the meteoroid. Thus the acceleration relative to the nucleus is given by

$$a = \frac{F_{drag}}{m_p} - \frac{GM_c}{l^2} \tag{2.4}$$

where m_p is the mass of the meteoroid particle, M_c the mass of the nucleus and G the universal gravitational constant. Thus the velocity at infinity relative to the nucleus is

$$\int_{v_o}^{v_\infty} V dV = \left(\frac{\Gamma \bar{v} A C_d}{4\pi m_p} - m_p G M_c \right) \int_{R_c}^{\infty} \frac{dl}{l^2} \tag{2.5}$$

or (assuming the initial velocity is zero):

$$v_\infty{}^2 = 2R_c \left[\frac{39 \bar{v} S}{72\ r^2 H \sigma \rho_m} - \frac{R_c 4\pi \rho_c G}{3} \right] \tag{2.6}$$

where ρ_c is the bulk density of the cometary nucleus, σ is the radius of the meteoroid and ρ_m the bulk density of the meteoroid. The 2nd term in Eq 2.6 is typically a few percent of the first term.

Jones (1995) and others (cf. Gustafson, 1989) have re-examined this problem and found very similar equations, producing ejection velocities from physically identical starting conditions within a few tens of percent of the Whipple value.

That this is only an approximation is made clear by cometary observations showing the presence of isolated jets, nucleus rotation, complex coma behaviour etc. In particular, Steel (1994) has noted the existence of distributed production (i.e. the concept that sublimation is not confined just to the surface of the nucleus, but rather each of the initial meteoroids contribute to sublimation immediately after release), inferred from the observations of Halley's comet, and has suggested that this may produce radically different ejection velocities than those traditionally used in the Whipple approach. This is indeed the case and is developed in more detail in Chapter 4.

To this point we have been concerned with defining the probable ejection speeds, location of ejections and the most likely direction of ejection for meteoroids. The preceding physical model provides an estimate of the ejection speed likely for a given mass, while cometary observations (see Chapter 4) suggest ejection of meteoroids is unlikely beyond ~4 A.U.. We can only surmise that ejection of meteoroids is most probable on the sunward hemisphere of the comet at any instant. Rotation of the nucleus, thermal lag and the existence of isolated active regions will modify this last statement, but information on individual cometary nuclei is insufficient in most cases to warrant making a more precise choice for ejection directions which would deviate from a simple sunward ejection location (chosen at random).

Once we define the ejection location and velocity relative to the nucleus, the initial unperturbed orbit of the individual meteoroid can be defined. It is the ensemble of these initial orbits, which form the initial meteoroid stream.

2.3 Initial orbit upon Ejection

From the previous section we anticipate ejection velocities <~100 m/s for meteoroids of the size range of interest (>10^{-5} g) (cf. Jones, 1995 for detailed examples).

For ejections within 4 A.U. of the Sun, typical cometary velocities are of order V ~ 30-40 km/s for highly eccentric orbits (such as the Leonids and Perseids - see Fig 2.1). Thus the ejection velocity of the meteoroid relative to the comet, v, is such that $v << V$ and

we denote the component of the velocity perpendicular to the cometary orbital plane and positive in the direction of the north cometary orbital "pole" as v_n, the component in the direction of the Sun as v_r and the component opposite the direction of the comet's instantaneous velocity vector as v_t. Fig 2.2 shows this right-handed coordinate system relative to the cometary orbit.

The total orbital energy per unit mass is given by (eg. Plavec, 1957):

$$E = T + U = \frac{v^2}{2} - \frac{\mu}{r} = -\frac{\mu}{2a} \tag{2.7}$$

where a is the osculating value of the semi-major axis, v is the heliocentric velocity, T is the kinetic energy, U is the potential energy and r is the heliocentric distance. μ represents GM_s where G is the universal gravitational constant and M_s the mass of the sun. For a particle ejected from the comet at r, its velocity relative to the comet causes a change in semi-major axis of

$$a_p = -\frac{2a^2}{\mu} V v_t + a \tag{2.8}$$

where a_p is the particle's semi-major axis immediately after ejection and we have assumed that $2Vv_t/\mu << 1$. The difference in semi-major axis (and thus energy) due to the velocity of ejection effectively depends on the magnitude of the meteoroid's ejection velocity parallel to the comet's velocity vector. The maximum change in semi-major axis is made when V is largest (i.e. at perihelion).

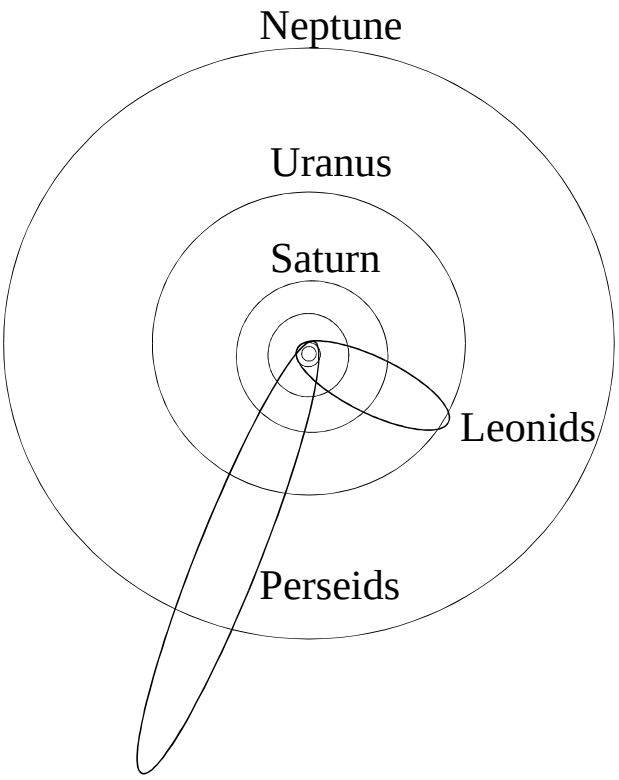

Fig 2.1: The orbits of the Leonid and Perseid meteoroid streams as seen from above the ecliptic plane of the solar system.

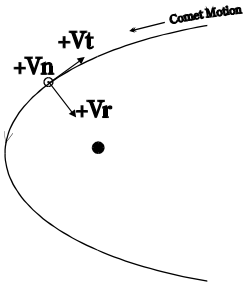

Fig 2.2: Cometocentric coordinate system for ejection of meteoroids. The normal component of the ejection velocity, v_n, is directed out of the page; v_r is positive in the direction of the sun, and v_t is positive in the direction opposite the comet's instantaneous velocity vector and is perpendicular to v_r.

It is possible to cast Eq 2.8 in a different form by making use of Kepler's third law and defining the fractional change in the period per revolution from ejection velocity as

$$\frac{dP}{P} = \frac{3a}{\mu} V v_t \tag{2.9}$$

In Fig 2.3 we show the expected fractional change in period resulting solely from ejection velocity for the Leonids and Perseids.

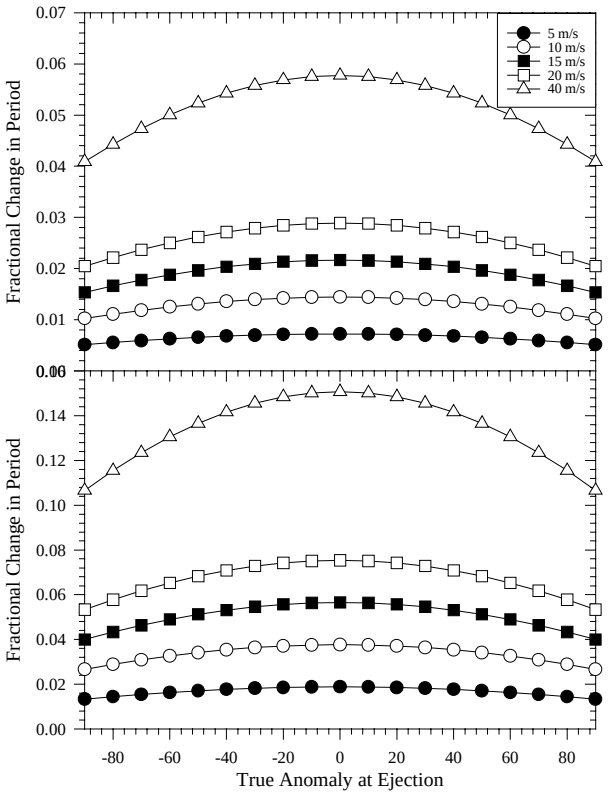

Fig 2.3: The fractional change in the orbital period for the Leonids (top) and Perseids (bottom) for ejection velocities from 5-40 m/s (see legend) for ejection at the given value of true anomaly. The change in period is calculated in steps of 10° of true anomaly.

Each of the orbital elements is similarly affected by the ejection velocity, but in a more complex fashion in a different manner and depending on the magnitude of each component. Pecina and Simek (1997) summarize these in detail but we note a few of physical interest here. The keplerian system of orbital elements is defined in Appendix A.

The change in the longitude of the ascending node Ω (which is a direct measure of when a given meteoroid is encountered during Earth's intersection with a stream) due to ejection velocity is given by

$$\Delta\Omega = \frac{\sqrt{a(1-e^2)}\sin(\theta+\omega)}{\mu^{\frac{1}{2}}(1+e\cos\theta)\sin i}\, v_n \qquad (2.10)$$

where θ is the true anomaly, ω is the argument of perihelion and i is the inclination of the initial orbit. Fig 2.4 shows the change in the longitude of the ascending node as a function of the normal component of the ejection velocity for various values of true anomaly for the Leonids. It is evident a larger change in Ω is accomplished the further from perihelion for any given value of v_n. Ejections near perihelion (and for Tempel-Tuttle slightly thereafter) have the least affect on the nodal longitude of the final orbit as the descending node is near perihelion.

For any meteoroid to actually intersect the Earth, its nodal radius (the point where it intersects the ecliptic) must be at the same distance from the sun as the Earth when the Earth is at the meteoroid's nodal longitude. This condition is

$$\frac{a(1-e^2)}{1\pm e\cos\omega} = Re \qquad (2.11)$$

where Re is the radius of the Earth's orbit at $\lambda(\Omega, \Omega+180°)$, the negative sign in the denominator of Eq. 2.11 is for the descending node and the positive sign is for the ascending node (where $\lambda=\Omega+180°$). By taking the differential of Eq. 2.10 (see Chapter 4) and using values for the osculating elements appropriate for the Perseids and Leonids we show directly the change in the descending node due to ejection velocity alone in Fig 2.5 a and b respectively. Typical ejection velocities of order 10-20 m/s in the orbital plane produce changes in the descending nodal radius of less than 10^{-3} A.U. for the Leonids near perihelion, while only slightly higher ejection velocities near 40 m/s produce an order of magnitude greater change (0.01 A.U.) for the less bound Perseid meteoroids. For

identical ejection velocities, Perseid meteoroid nodal radius differences are three to five times larger on average than those of Leonid meteoroids (depending on location of ejection).

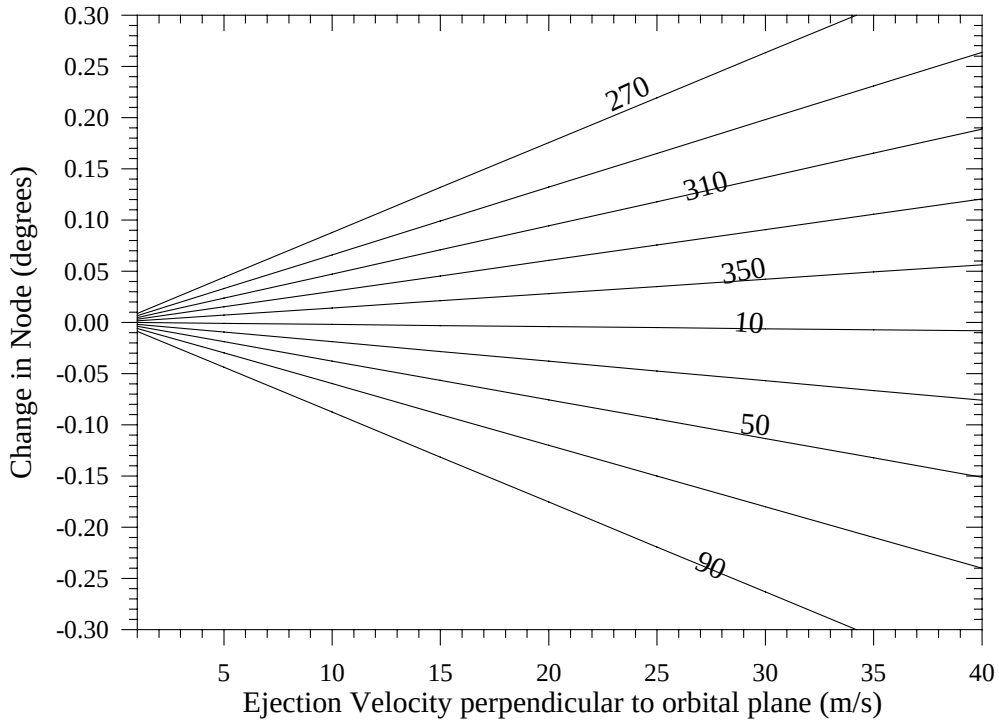

Fig 2.4: Change in the osculating value of the ascending node (Ω) for ejection from 55P/Tempel-Tuttle as a function of the normal component of the velocity (V_n) at different values of true anomaly from 270°-90° in 20° steps.

For comparison, the change in the nodal radius due to radiation pressure affects alone for the Leonids and Perseids (see next section) is shown in Fig 2.6. For both orbits, the effect is much smaller than that of ejection velocities, even for very small particles.

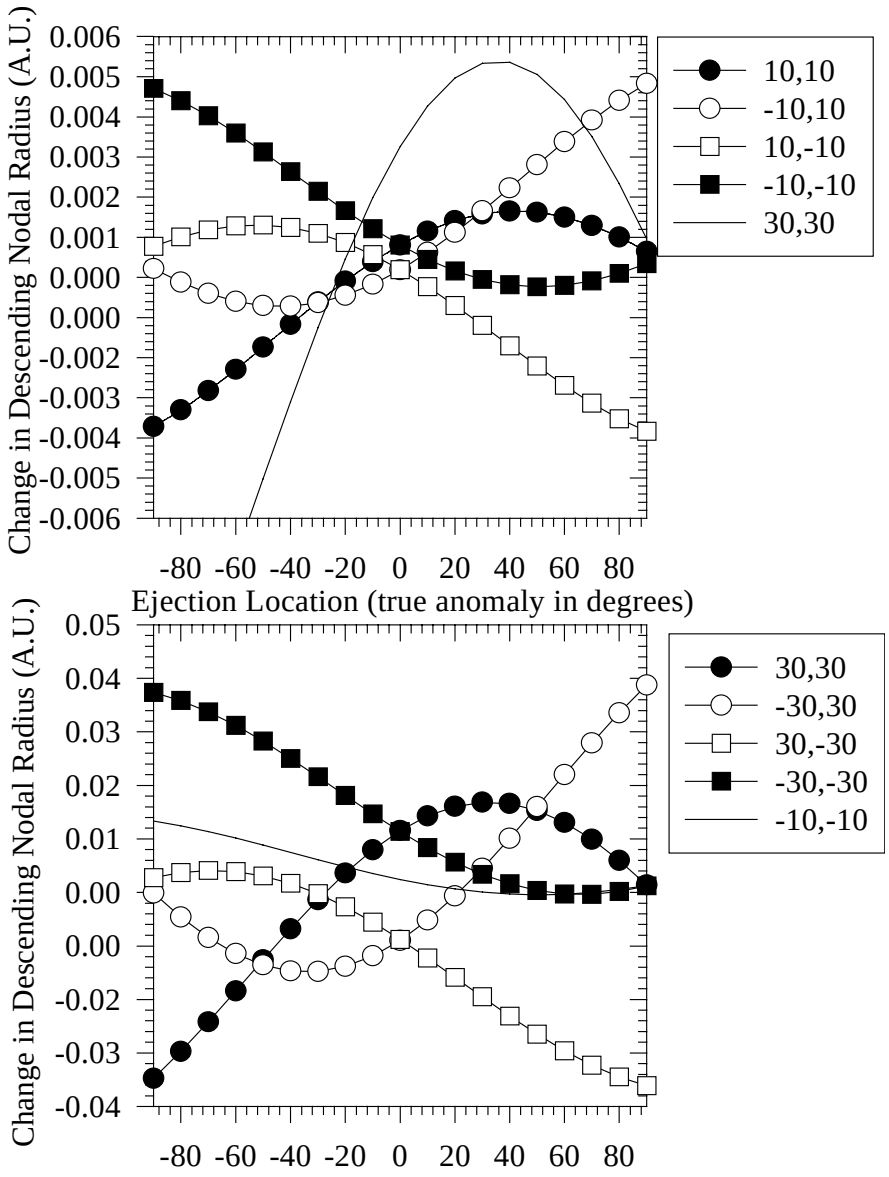

Fig 2.5: Change in the magnitude of the descending nodal radius as a function of ejection velocity and true anomaly of ejection for the Leonids (top) and Perseids (bottom). The legend shows the radial, transverse ejection velocity component pairs in units of m/s. Note that the ejections are assumed to be confined to the orbital plane (i.e. V_n=0).

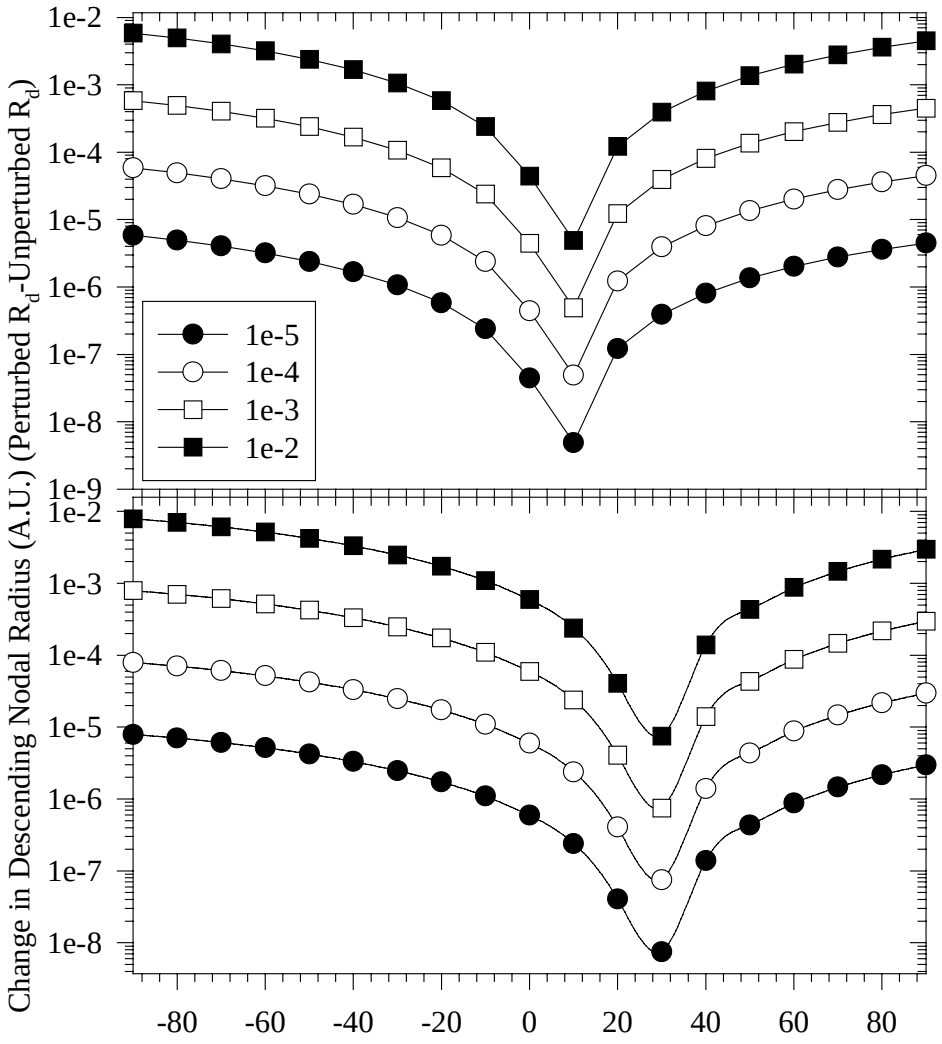

Fig 2.6: Change in the magnitude of the heliocentric radius of the descending node for the Leonids (top) and Perseids (bottom) resulting from radiation pressure as a function of position (in true anomaly) of release. The change is shown assuming a zero net ejection velocity. The legend gives values for β (defined in Chapter 3) associated with each curve. Note that the nodal radius affected by radiation pressure is always larger than the original nodal radius. Values are computed in steps of 10°.

2.4 Forces acting on the meteoroid after ejection

Immediately after ejection, the initial orbit established in Sect. 2.3 is modified by numerous forces (cf. Burns et al., 1979). In total, the relevant forces acting on a meteoroid of order 10^{-5} g and larger after ejection are given by

$$F = \frac{-GM_s}{|r|^2} mr + \sum_{i=1}^{9} Gm\left[\frac{m_i}{|r - r_i|^3}(r - r) + \left(\frac{m_i \mathrm{M_s}}{M_s + m_i} \right) \frac{r_i}{|r_i|^3} \right]$$
$$+ \frac{SA}{c} r - \frac{SA}{c^2}(2V_r - V_t) + \frac{8\pi s^2}{3c} \sigma T^4 \frac{\Delta T}{T} \cos\varsigma \qquad (2.12)$$

where the summation is over all planets from Mercury to Pluto; r is the radius vector from the sun to the meteoroids, r_i and m_i are the radius vector and mass of planet i; M_s is the mass of the sun, m the mass of the meteoroid; S is the solar flux at distance r (in A.U.) from the sun ($S=1.37/r^2$ in units of kW m^{-2}); A is the cross-sectional area of the meteoroid relative to the solar direction; c is the speed of light; V_r and V_t are the radial and transverse heliocentric velocities of the meteoroid respectively; s is the physical radius of the meteoroid; σ is the Stefan-Boltzmann constant; T is the mean temperature of the meteoroid; ΔT is the temperature differential across the meteoroid surface and ζ is the obliquity of the spin axis of the meteoroid relative to the orbital normal direction.

Eq. 2.12 is composed of six terms, each representing a separate physical force acting on the meteoroid, with the approximate relative importance of the forces decreasing approximately from left to right.

The first term represents the radial attraction of the sun and is by far the strongest of the forces acting on the meteoroid (the central force). The meteoroid's motion is defined in heliocentric terms, as this motion is an excellent approximation of a two-body system (sun-meteoroid).

The second term consists of the summation of the direct gravitational attraction of each of the planets. The specific terms of importance here depend to a great extent on the meteoroid's orbit, but typically Jupiter and/or Saturn dominate (see discussions in Chapters 4 and 6 relative to the Perseids and Leonids).

The third term is often referred to as indirect planetary perturbations or the barycentric correction term. This force is analogous to the (fictitious) centrifugal force in uniform circular motion and is purely a result of the choice of a non-inertial coordinate system. Physically, the meteoroid does not move about the sun (though we reference it to the center of the sun) but rather about the center of mass of the solar system. This point (called the barycenter) is slightly offset from the center of the sun, due primarily to the attraction of Jupiter and (to a lesser degree) Saturn. It also moves relative to the solar center depending on the position of the major planets. As a result, the heliocentric orbital elements appear to "wobble" in direct relation to the acceleration of the barycenter relative to the solar center. This force becomes more significant for objects with very eccentric orbits near aphelion, since the force is independent of the distance of the meteoroid from the sun and hence has greatest effect when the object is least bound to the sun (i.e. has the highest potential energy). The relative importance of the effect decreases as the object moves inward, becoming insignificant once the object is interior to Jupiter. The indirect perturbations are also typically smaller than the effects of distant (1-2 A.U.) direct perturbations from the major planets (see Chapter 6). Chambers (1995) has discussed the role of indirect perturbations in maintaining resonance behaviour in Halley-type comets and provides an excellent discussion of the role of the force for such highly eccentric orbits.

The fourth term in Eq. 2.12 is due to solar radiation pressure. Photons from the Sun carry momentum with them. When the meteoroid absorbs incident solar photons it removes momentum from the particle beam. This rate of change of momentum (a force) in the beam, as seen from the meteoroid, acts on the meteoroid in direct proportion to the exposed geometric surface area and its scattering efficiency. For a perfectly absorbing particle, the scattering efficiency is unity and we adopt this throughout. The force acts radially away from the Sun as the momentum of the incident photons is virtually all in this direction.

As this force is radial and falls off as $1/r^2$, like the central gravitational attraction of the Sun, it is often included with the central force term. More specifically, it is common to refer to the (constant) ratio of radiation force to gravitational force as $\beta=F_r/F_g$

or $\beta=5.7\times10^{-6}/\rho s$, where ρ is the bulk density of the meteoroid and s the radius in MKS units. In this manner it is possible to recast the radiation force and gravitational force as

$$\vec{F} = GM(1-\beta)\frac{\vec{r}}{|\vec{r}|^3} \tag{2.13}$$

which makes it clear that the effect of radiation pressure is equivalent to a decrease in the central force (i.e. an effective decrease in the sun's mass). As the radiation pressure (which is typically the dominant radiation force for meteoroids of the size we are considering) acts immediately upon ejection (that is, it immediately begins moving under the new, effectively reduced central potential), while retaining its pre-release orbital velocity, it is straightforward to show that from energy considerations, a pre-ejection bound orbit can become unbound for ejection at true anomaly θ if the condition

$$\beta \geq \frac{1-e^2}{2(1+e\cos\theta)} \tag{2.14}$$

is met. Thus, the value of β that is required for very eccentric orbits ($e\rightarrow1$) to become unbound is quite low (much less than 1). For ejection at perihelion (when the meteoroid and parent body are moving at their highest speeds relative to the Sun and the energy in the body is partitioned primarily into kinetic energy), a Leonid meteoroid with a value of $\beta > 0.05$ is unbound while for a Perseid the value is only 0.02.

The fifth term is due to radiation emission by the meteoroid. As radiation falls on the meteoroid it is re-emitted isotropically in the meteoroid's rest frame at the sizes we are concerned with. However, since the meteoroid is moving with non-zero velocity about the sun, the radiation emitted from its leading edge is doppler-shifted (towards the blue) relative to the radiation from its trailing edge. As a result, the force imparted to the particle from the blue-shifted light (which has higher momentum than red-shifted light) acts in the direction opposite to the leading edge (away from the instantaneous velocity vector) and works to "brake" the particle. This force is called the Poynting-Robertson (PR) effect (cf. Burns et al, 1979 for both a classical and relativistic treatment of this force).

From Eq. 2.12 it is clear that the PR effect is of order v/c (typically $\sim10^{-4}$) relative to radiation pressure and is thus negligible for particle dynamics over the short time

periods or the larger meteoroids we investigate. The PR effect becomes significant only over long time intervals, cumulatively removing momentum and energy from a small meteoroid (of order μm in size) such that the orbit circularizes and the semi-major axis decreases, allowing the particle to move into regimes where other dynamics (such as planetary resonances) can affect it (cf. Liou and Zook, 1997).

The last term in Eq. 2.12 is the most difficult to measure physically and its relative importance has been debated for some time (eg. Olsson-Steel, 1987). It arises from the non-isotropic re-emission of radiation for a spinning non-isothermal body. In this scenario, extra radiation and energy (as well as momentum) are emitted in the "evening" hemisphere relative to the "morning" hemisphere due to the temperature difference between the two. Depending on the orientation of the rotation axis and the sense of the spin, this radiation emission imbalance can lead to forces, which act, on the meteoroid in any direction. As a result, unlike radiation pressure or the PR effect, this force (called the Yarkovsky-Radzievskii effect) is diffusive in nature and leads to a random-walk in the perturbed meteoroid motion. The direction in which the force acts depends on the orientation of the rotation axis. None of these quantities is known with high degrees of confidence for typical meteoroids. As a result, it is possible that in the extreme case of slow rotating objects, the Yarkovsky force may be 10^3-10^4 times that of the PR force, though the random direction of the force mitigates its role compared to the smaller but consistent drag from the PR effect. Even in this extreme case, however, the Yarkovsky effect is still only a fraction of a percent (and usually much less) of radiation pressure for meteoroids of the size range studied here. The real importance of the effect may be felt over long time periods and for very large bodies (cf. Bottke et al., 1998). As a result we do not include the Yarkovsky force in any of our numerical calculations, noting that over a few centuries (where most of our integrations are concerned) it is unlikely to be of significance.

References

Bottke, W. D.L.Rubincam and J.A. Burns, 1998. Dynamical Evolution of Meteoroids via the Yarkovsky Effect, American Astronomical Society, DPS meeting #30.

Burns, J.A. P.L. Lamy and S. Soter, 1979. Radiation forces on small particles in the solar system, *Icarus*, **40**, 1.

Ceplecha, Z., J. Borovicka, W.G. Elford, D.O. Revelle, R.L. Hawkes, V. Porubcan, and M Simek, 1998. Meteor Phenomena and Bodies, *Sp.Sci. Rev.*, 84, 327-471.

Chambers, J.E. 1995. The long term dynamical evolution of comet Swift-Tuttle. *Icarus* **114**, 372-386.

Crifo, J.F. and A.V. Rodionov, 1999, Modelling the circumnuclear Coma of Comets: Objectives, Methods and Recent Results, in press.

Finson, M.L. and R.F. Probstein, 1968. A theory of dust comets. I. Model and equations, *ApJ*., **153**, 353.

Greenberg, J.M. and J.I. Hage. 1990. From Interstellar Dust to Comets:A Unification of Observational Constraints, *ApJ*, 361, 260-274.

Gustafson, B.A.S. 1989. Comet Ejection and Dynamics of Nonspherical dust Particles and meteoroids. *Ap.J.* **337**, 945-949.

Jones, J. 1995. The ejection of meteoroids from comets. *Mon. Not. R. Astron. Soc*. **275**, 773-780.

Liou, J-C. and H. Zook. 1997. Evolution of Interplanetary Dust Particles in Mean Motion Resonances with Planets, *Icarus*, **128**, 354.

Olsson-Steel, D. 1987. The dispersal of meteoroid streams by radiative effects, in *10th European Regional Astronomy Meeting of the IA.U.*, Prague, Czechoslovakia, Aug. 24-29, 1987, p. 157-161

Pecina, P. and M. Simek. 1997. The orbital elements of a meteoroid after its ejection from a comet, *A&A*, **317**, 594-600.

Plavec, M. 1957. *On the Origin and Early Stages of the Meteor Streams*, Czechoslovak Academy of Sciences, Publication No. 30., Prague.

Steel, D. 1994. Meteoroid Streams, in *Asteroids, Comets, Meteors 1993*, (eds. A. Milani et al.), p. 111-126, IA.U..

Weidenschilling, S.J. 1988. Formation processes and time scales for meteorite parent bodies, in *Meteorites and the Early Solar System*, (eds. J.F. Kerridge and M.S. Matthews), p.348-375, University of Arizona.

Whipple, F.L. 1951. A comet model II. Physical relations for comets and meteors. *AJ* **113**, 464-474.

Williams, I.P. 1993, The dynamics of Meteoroid Streams, In *Meteoroids and Their Parent Bodies* (J. Štohl and I. P. Williams, Eds.), p. 31-40. Astronomical Inst., Slovak Acad. Sci., Bratislava.